Excited State Localization and Internuclear Interactions in Asymmetric Ruthenium(II) and Osmium(II) bpy/tpy Based Dinuclear Compounds

Yvonne Halpin,[†] Danilo Dini,[†] Hamid M. Younis Ahmed,[†] Lynda Cassidy,[†] Wesley R. Browne,[‡] and Johannes G. Vos*,[†]

[†]*Solar Energy Conversion SRC, School of Chemical Sciences, Dublin City University, Dublin 9, Ireland, and* [‡]*Center for Systems Chemistry, Stratingh Institute for Chemistry and Zernike Institute for Advanced Materials, Faculty of Mathematics and Natural Sciences, University of Groningen, Nijenborgh 4, 9747AG Groningen, The Netherlands*

The synthesis of two asymmetric dinuclear complexes with the formula [M(bpy)$_2$(bpt)Ru(tpy)Cl]$^{2+}$, where M = Ru (**1a**), Os(**2a**); bpy = 2,2′-bipyridyl; Hbpt = 3,5-bis(pyridin-2-yl)1,2,4-triazole and tpy = 2,2′,6′,2′′-terpyridine, is reported. The compounds obtained are characterized by mass spectrometry, ^{1}H NMR, UV/vis/NIR absorption, luminescence, and resonance Raman spectroscopy. Deuterium isotope labeling facilitates assignment of the ^{1}H NMR and resonance Raman spectra. The interaction between the two metal centers, mediated by the bridging 1,2,4-triazolato moiety in the mixed valent state, is assigned as type II based on the observation of metal to metal charge transfer absorption bands at 7090 and 5990 cm^{-1} for **1a** and **2a**, respectively. The extent of localization of the emissive excited state was determined by transient resonance Raman and emission spectroscopy. Both **1a** and **2a** show phosphorescence at the same wavelengths; however, whereas for compound **1a** the emission is based on the Ru(tpy)Cl- center, for **2a** the emissive state is localized on the Os(bpy)$_2$- unit. This indicates that also in the excited state there is efficient interaction between the two metal centers.

Introduction

The remarkable combination of spectroscopic and electrochemical properties of ruthenium and osmium based polypyridyl complexes,[1,2] which can be tuned in a predictable manner synthetically and by electrochemical oxidation or reduction, has led to their widespread application to molecular machines,[3] dye-sensitized solar cells,[4] electro- and optical sensors,[5] chemiluminescent devices[6] and electrochromic displays,[7] and have proven invaluable in the development of nonlinear optics,[8] artificial photosynthesis,[9] and molecular electronics.[10] Multinuclear metal polypyridyl complexes are of particular interest in regard to transfer either electronic charge or excitation from one site of coordination to the other via π-delocalized bridging ligands manifested in near-infrared (NIR) absorptions.[11] In principle, such intramolecular charge transfer in binuclear complexes can be exploited

*To whom correspondence should be addressed. E-mail: han.vos@dcu.ie. Fax: 00353 1 700 5503. Phone: 00353 1 700 5307.

(1) (a) Juris, A.; Balzani, V.; Barigelletti, F.; Campagna, S.; Belser, P.; von Zelewsky, A. *Coord. Chem. Rev.* **1988**, *84*, 85–277. (b) Lytle, F. E.; Hercules, D. M. *J. Am. Chem. Soc.* **1969**, *91*, 253–257.

(2) Vos, J. G.; Kelly, J. M. *Dalton Trans.* **2006**, 4869–4883.

(3) (a) Balzani, V.; Bergamini, G.; Ceroni, P. *Coord. Chem. Rev.* **2008**, *252*, 2456–2469. (b) Balzani, V.; Bergamini, G.; Marchioni, F.; Ceroni, P. *Coord. Chem. Rev.* **2006**, *250*, 1254–1266.

(4) (a) O'Regan, B.; Grätzel, M. *Nature* **1991**, *353*, 737–740. (b) Hagfeldt, A.; Grätzel, M. *Acc. Chem. Res.* **2000**, *33*, 269–277.

(5) (a) Rajagopalan, C. R.; Aoki, A.; Heller, A. *J. Phys. Chem.* **1996**, *100*, 3719–27. (b) Doherty, A. P.; Stanley, M. A.; Leech, D.; Vos, J. G. *Anal. Chim. Acta* **1996**, *319*, 111–120. (c) Doherty, A. P.; Vos, J. G. *J. Chem. Soc., Faraday Trans.* **1992**, *88*, 2903–2907. (d) Demas, J. N.; DeGraff, B. A. *Anal. Chem.* **1991**, *63*, 829A–837A. (e) Lippitsch, M. E.; Pusterhofer, J.; Leiner, M. J. P.; Wolfbeis, O. S. *Anal. Chim. Acta* **1988**, *205*, 1–6. (f) Demas, J. N; DeGraff, B. A. *Chem. Educ.* **1997**, *74*, 690–695. (g) Malins, C.; Fanni, S.; Glever, H. G.; Vos, J. G.; MacCraith, B. D. *Anal. Commun.* **1999**, *36*, 3–4.

(6) (a) Chen, C. H.; Shi, J. M. *Coord. Chem. Rev.* **1998**, *171*, 161–174. (b) Armstrong, N. R.; Wightman, R. M.; Gross, E. M. *Annu. Rev. Phys. Chem.* **2001**, *52*, 391–422.

(7) (a) Marcaccio, M.; Paolucci, F.; Paradisi, C.; Roffia, S.; Fontanesi, C.; Yellowlees, L. J.; Serroni, S.; Campagna, S.; Denti, G.; Balzani, V. *J. Am. Chem. Soc.* **1999**, *121*, 10081–91. (b) Stagni, S.; Palazzi, A.; Zacchini, S.; Ballarin, B.; Bruno, C.; Marcaccio, M.; Paolucci, F.; Monari, M.; Carano, M.; Bard, A. J. *Inorg. Chem.* **2006**, *45*, 695–709. (c) Marcaccio, M.; Paolucci, F.; Paradisi, C.; Carano, M.; Roffia, S.; Fontanesi, C.; Yellowlees, L. J.; Serroni, S.; Campagna, S.; Balzani, V. *J. Electroanal. Chem.* **2002**, *532*, 99–112. (d) Roffia, S.; Casadei, R.; Paolucci, F.; Paradisi, C.; Bignozzi, C. A.; Scandola, F. *J. Electroanal. Chem.* **1991**, *302*, 157–171.

(8) (a) Feuvrie, C.; Maury, O.; Le Bozec, H.; Ledoux, I.; Morrall, J. P.; Dalton, G. T.; Samoc, M.; Humphrey, M. G. *J. Phys. Chem. A* **2007**, *111*, 8980–8985. (b) Girardot, C.; Cao, B.; Mulatier, J. C.; Baldeck, P. L.; Chauvin, J.; Riehl, D.; Delaire, J. A.; Andraud, C.; Lemercier, G. *ChemPhysChem* **2008**, *9*, 1531–1535. (c) Maury, O.; Le Bozec, H. *Acc. Chem. Res.* **2005**, *38*, 691–704.

(9) Sun, L.; Hammarström, L.; Åkermark, B.; Styring, S. *Chem. Soc. Rev.* **2001**, *30*, 36–49.

(10) Albrecht, T.; Moth-Poulsen, K.; Christensen, J. B.; Guckian, A.; Bjornholm, T.; Vos, J. G.; Ulstrup, J. *Faraday Discuss.* **2006**, *13*, 265–279 and references therein.

(11) Balzani, V.; Juris, A.; Venturi, A.; Campagna, S.; Serroni, S. *Chem. Rev.* **1996**, *96*, 759–833.
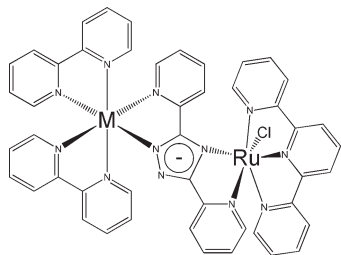
Figure 1. Structure of dinuclear complexes **1a** (M = Ru) and **2a** (M = Os).

for the realization of miniaturized sub-nanoscale devices where electrons or photons dispatch "information" between specific sites within distances of the order of a few angstroms.[12] A key challenge therefore is to be able to control not only the strength of the interaction between the two metal centers in both the ground and the excited state but also the direction. This can be achieved through the structural modification of the bridging ligand and the variation of the nature of the coordinating metal centers. In this regard dinuclear complexes bridged by negatively charged 1,2,4-triazolato moieties including homonuclear and heteronuclear 2,2′-bipyridyl based Ru(II) and Os(II) complexes[13−20] as well as cyclometalated complexes based on Rh and Ir[21] have been investigated by our group over recent years, in particular with respect to the ground state and excited state intercomponent interaction.

Here we report the synthesis and characterization of two binuclear complexes of ruthenium and osmium, containing both bpy (2,2′-bipyridine) and tpy (2,6-bis(pyridin-2′-yl)-pyridine) as peripheral ligands of the general formula [(bpy)$_2$-M(bpt)Ru(tpy)Cl]$^{2+}$ where M = Ru (**1a**) and Os (**2a**) (Figure 1). In compounds **1a** and **2a** the bridging ligand 3,5-bis(pyridin-2′-yl)-1,2,4-triazolato (bpt) is negatively charged. In contrast to related pseudo-symmetric systems,[13,14] in **1a** and **2a** the non-bridging polypyridyl ligands at each center are geometrically and photophysically distinct, that is, (bpy)$_2$ versus (tpy)Cl. The extent and directionality of the interaction between the triazolato bridged metal centers is found to be highly dependent on the nature of the metal center. The corresponding deuterated isotopologues [(d$_8$-bpy)$_2$M(bpt)-Ru(tpy)Cl]$^{2+}$ [M = Ru (**1b**), Os (**2b**)] were prepared to facili-

tate assignment of the chemical shifts of the protons in the bridging bpt- ligand and tpy peripheral ligand as well as the vibrational and electronic spectroscopic features. The results obtained show that in these systems the location of the lowest emissive excited state and the first oxidation can be switched by judicious choice of the metal centers. Importantly this can be done with only minimal perturbation of the photophysical properties including electronic absorption and emission spectra.

Experimental Section

Materials. All solvents employed in spectroscopic measurements were of spectroscopic grade (Sigma-Aldrich). All other solvents were of HPLC grade or better. cis-Ru(bpy)$_2$Cl$_2$·2H$_2$O,[22] Ru(d$_8$-bpy)$_2$Cl$_2$·2H$_2$O, Os(bpy)$_2$Cl$_2$[23] and Ru(tpy)Cl$_3$,[24] d$_8$-bpy[25] and 3,5-bis(pyridin-2-yl)-1,2,4-triazole (Hbpt)[26] were prepared by reported procedures. Gold colloid for SERS measurements was prepared by standard methods.[27]

The syntheses of the mononuclear complexes were as reported in the literature.[13]

[Ru(bpy)$_2$(bpt)](PF$_6$)·1/2H$_2$O: Yield: 92 mg (0.12 mmol), 51%, ^{1}H NMR (CD$_3$CN, 298 K) δ/ppm: 8.53 (1H, d), 8.43 (4H, m), 8.15 (1H, d), 7.92 (8H, m), 7.90 (1H, d), 7.83 (1H, dd), 7.75 (1H, dd), 7.52 (1H, d), 7.37 (4H, m), 7.23 (1H, dd), 7.14 (1H, dd). Elemental analysis for C$_{32}$H$_{24}$N$_9$RuPF$_6$·1/2H$_2$O: Calcd: C 48.7%, H 3.17%, N 15.96%. Found: C 48.4%, H 3.22%, N 15.91%.

[Ru(d$_8$-bpy)$_2$(bpt)](PF$_6$)·1/2H$_2$O: Yield: 55 mg (0.06 mmol), 31%, ^{1}H NMR (CD$_3$CN, 298 K) δ/ppm: 8.50 (1H, d), 8.15 (1H, d), 8.01 (1H, d), 7.90 (1H, t), 7.70 (1H, t), 7.55 (1H, d), 7.20 (1H, t), 7.15 (1H, t). Elemental analysis for C$_{32}$H$_8$D$_{16}$N$_9$RuPF$_6$·1/2H$_2$O: Calcd: C 47.7%, H 3.10%, N 15.65%. Found: C 48.4%, H 2.97%, N 15.49%.

[Os(bpy)$_2$(bpt)](PF$_6$)·2H$_2$O. 82 mg (0.09 mmol), 43%, ^{1}H NMR (CD$_3$CN, 298 K) δ/ppm: 8.55 (1H, d), 8.43 (4H, m), 8.18 (1H, d), 7.92 (8H, m), 7.95 (1H, d), 7.88 (1H, dd), 7.65 (1H, dd), 7.40 (1H, d), 7.15 (1H, dd), 7.37 (4H, m), 7.05 (1H, dd). Elemental Analysis for C$_{32}$H$_{24}$N$_9$OsPF$_6$·2H$_2$O: Calcd: C 42.4%, H 3.09%, N 13.92%. Found: C 42.9%, H 3.08%, N 13.80%.

[Os(d$_8$-bpy)$_2$(bpt)](PF$_6$)·2H$_2$O. Yield: 16 mg (0.02 mmol), 9%, ^{1}H NMR (CD$_3$CN, 298 K) δ/ppm: 8.55 (1H, d), 8.15 (1H, d), 8.01 (1H, d), 7.75 (1H, dd), 7.72 (1H, d), 7.42 (1H), 7.25 (1H, dd), 7.15 (1H, dd). Elemental analysis for C$_{32}$H$_8$D$_{16}$N$_9$OsPF$_6$·2H$_2$O: Calcd: C 41.7%, H 3.04%, N 13.68%. Found: C 41.6%, H 2.95%, N 13.62%.

Ru(tpy)Cl$_3$. A 981 mg portion (4.1 mmol) of RuCl$_3$·2H$_2$O was dissolved in 150 cm^3 of ethanol, the solution was refluxed and 1 equiv of 2,2′;6′,2″ terpyridine (tpy), dissolved in 20 cm^3 of ethanol, were dropped in the reaction bulk. The reaction mixture was heated for 2 h and filtered hot. A dark solid was collected and washed with ethanol, water, and diethyl ether. Yield: 681 mg (1.6 mmol), 80%.

Synthesis of Dinuclear Complexes. [Ru(bpy)$_2$(bpt)Ru(tpy)-Cl](PF$_6$)$_2$·2H$_2$O (1a). Ru(tpy)Cl$_3$ (100 mg, 0.13 mmol) was dissolved in 10 cm^3 ethanol/water (1:1 v/v). [Ru(bpy)$_2$(bpt)]PF$_6$·1/2H$_2$O (119 mg, 0.13 mmol) was added, and the mixture was left to heat at reflux for 8 h. The reaction was cooled to room

(12) (a) D'Alessandro, D. M.; Keene, F. R. Pure Appl. Chem. **2008**, 80, 1–16. (b) D'Alessandro, D. M.; Keene, F. R. Chem. Rev. **2006**, 106, 2270–2298. (c) Launay, J. P. Chem. Soc. Rev. **2001**, 30, 386–397.
(13) Hage, R.; Dijkhuis, A. H. J.; Haasnoot, J. G.; Prins, R.; Reedijk, J.; Buchanan, B. E. Vos, J. G. Inorg. Chem. **1988**, 27, 2185–2189.
(14) Hage, R.; Haasnoot, J. G.; Nieuwenhuis, H. A.; Reedijk, J.; De Ridder, D. J. A.; Vos, J. G. J. Am. Chem. Soc. **1990**, 112, 9245–9251.
(15) De Cola, L.; Barigelletti, F.; Balzani, V.; Hage, R.; Haasnoot, J. G.; Reedijk, J.; Vos, J. G. Chem. Phys. Lett. **1991**, 178, 491–496.
(16) Di Pietro, C.; Serroni, S.; Campagna, S.; Gandolfi, T.; Ballardini, R.; Fanni, S.; Browne, W. R.; Vos, J. G. Inorg. Chem. **2002**, 41, 2871–2878.
(17) Browne, W. R.; Weldon, F.; Guckian, A.; Vos, J. G. Collect. Czech. Chem. Commun. **2003**, 68, 1467–1486.
(18) Weldon, F.; Hammarström, L.; Mukhtar, E.; Hage, R.; Gunneweg, E.; Haasnoot, J. G.; Reedijk, J.; Browne, W. R.; Guckian, A. L.; Vos, J. G. Inorg. Chem. **2004**, 43, 4471–4481.
(19) Hage, R.; Haasnoot, J. G.; Reedijk, J.; Wang, R.; Vos, J. G. Inorg. Chem. **1991**, 30, 3263–3269.
(20) Hage, R.; Lempers, H. E. B.; Haasnoot, J. G.; Reedijk, J.; Weldon, F. M.; Vos, J. G. Inorg. Chem. **1997**, 36, 3139–3145.
(21) (a) Van Diemen, J. H.; Haasnoot, J. G.; Hage, R.; Reedijk, J.; Vos, J. G.; Wang, R. Inorg. Chem. **1991**, 30, 4038–4043. (b) Van Diemen, J. H.; Hage, R.; Haasnoot, J. G.; Lempers, H. E. B.; Reedijk, J.; Vos, J. G.; De Cola, L.; Barigelletti, F.; Balzani, V. Inorg. Chem. **1992**, 31, 3518–3522.

(22) Sullivan, B. P.; Salmon, D. J.; Meyer, T. J. Inorg. Chem. **1978**, 17, 3334–3341.
(23) Lay, P. A.; Sargeson, A. M.; Taube, H.; Chou, M. H.; Creutz, C. Inorg. Synth. **1986**, 24, 291–299.
(24) Constable, E. C.; Thompson, A. M. W. C.; Tocher, D. A.; Daniels, M. A. M. New J. Chem. **1992**, 16, 855–867.
(25) Browne, W. R.; O'Connor, C. M.; Killeen, J. S.; Guckian, A. L.; Burke, M.; James, P.; Burke, M.; Vos, J. G. Inorg. Chem. **2002**, 41, 4245–4251.
(26) Geldard, J. F.; Lions, F. J. Org. Chem. **1965**, 30, 318–319.
(27) Lee, P. C.; Meisel, D. J. Phys. Chem. **1982**, 86, 3391–3395.

temperature and evaporated to dryness after which 10 cm^3 water was added, followed by precipitation of the product by the addition of aqueous NH$_4$PF$_6$. The product was isolated by filtration, washed with water and diethyl ether, and dried under vacuum. **1a** was isolated by column chromatography (stationary phase silica, mobile phase 80:20, acetonitrile:water, 0.05 M KNO$_3$). The compound was obtained after precipitation with aqueous NH$_4$PF$_6$ and subsequent recrystallization from acetone/water 1:1. Yield: 40 mg (0.04 mmol), 33%. ^{1}H NMR (CD$_3$CN, 298 K) δ/ppm: 10.08 [1H, d, H6(B)], 8.75 [1H, d, H3(B)], 8.70 [1H, d, H3'], 8.65 [5H, md, H3(1), H3'(1), H3(2), H3'(2), H3''], 8.47 [1H, d, H3], 8.20 [3H, m, H4', H5', H4(B)], 7.99 [3H, m, H4'', H6'', H4], 7.92 [2H, t, H4(1), H4'(2)], 7.72−7.81 [4H, md, H4(2), H4'(1), H5(B), H6], 7.60 [1H, t, H5''], 7.56 [1H, d, H6(A)], 7.51 [1H, d, H6(1)], 7.23−7.37 [5H, dm, H6'(2), H6'(1), H6(2), H5, H4(A)], 7.08−7.19 [4H, m, H5(1), H5'(1), H5(2), H5'(2)], 7.02 [1H, t, H5(A)], 6.47 [1H, d, H3(A)]. MS. Found: 502.5 (M^{2+}); Calcd: 502. Elemental Analysis for Ru$_2$-C$_{47}$H$_{35}$N$_{12}$ClP$_2$F$_{12}$·2H$_2$O: Calcd: C 42.4%, H 2.93%, N 12.62%. Found: C 42.4%, H 2.95%, N 12.53%.

[Ru(d$_8$-bpy)$_2$(bpt)Ru(tpy)Cl](PF$_6$)$_2$·2H$_2$O (1b). Yield: 15 mg (0.01 mmol), 11.5%. ^{1}H NMR (CD$_3$CN, 298 K) δ/ppm: 10.05 [1H, d, H6(B)], 8.78 [1H, d, H3(B)], 8.67 [1H, d, H3'], 8.58 [1H, d, H3''], 8.45 [1H, d, H3], 8.15 [3H, m, H4', H5', H4(B)], 7.95 [3H, m, H4'', H6'', H4], 7.79 [1H, m, H5(B)], 7.72 (1H, d, H6), 7.58 [1H, t, H5''], 7.53 [1H, d, H6(A)], 7.24 [2H, m, H5, H4(A)], 6.96 [1H, t, H5(A)], 6.43 [1H, d, H3(A)]. MS. Found 510 (M^{2+}); Calcd: 510. Elemental analysis for Ru$_2$C$_{47}$H$_{19}$D$_{16}$ N$_{12}$ClP$_2$F$_{12}$·2H$_2$O: Calcd: C 41.9%, H 2.89%, N 12.47%, Found: C 41.8%, H 2.97%, N 12.33%.

[Os(bpy)$_2$(bpt)Ru(tpy)Cl](PF$_6$)$_2$·H$_2$O (2a). Yield: 10 mg (0.01 mmol), 8%. ^{1}H NMR in CD$_3$CN at 298 K, δ/ppm: 10.01 [1H, d, H6(B)], 8.69 [1H, d, H3(B)], 8.52 [1H, d, H3'], 8.37−8.45 [5H, md, H3(1), H3'(1), H3(2), H3'(2), H3''], 8.27−8.35 [1H, d, H3], 8.15−8.25 [2H, m, H4', H5'], 8.08−8.15 [1H, t, H4(B)], 8.00−8.07 [2H, m, H4(1), H4'(2)], 7.80−7.99 [5H, m, H4'(1), H4(2), H4'', H6'', H4], 7.65−7.80 [2H, m, H5(B), H6(1)], 7.58−7.65 [1H, d, H6], 7.45−7.52 [1H, t, H5''], 7.40−7.45 [1H, d, H6(A)], 7.26−7.37 [4H, m, H6(2), H6'(1), H5(1), H4(A)], 7.15−7.24 [2H, m, H6'(2), H5'(2)], 7.01−7.22 [3H, t, H5, H5'(1), H5(2)], 7.00−7.05 [1H, t, H5(A)], 6.35−6.46 [1H, d, H3(A)]. MS. Found: 548.2 (M^{2+}); Calcd: 548. Elemental analysis for OsRuC$_{47}$H$_{35}$N$_{12}$ClP$_2$F$_{12}$·H$_2$O: Calcd: C 40.2%, H 2.64%, N 11.98%. Found: C 40.5%, H 2.75%, N 12.01%.

[Os(d$_8$-bpy)$_2$(bpt)Ru(tpy)Cl](PF$_6$)$_2$·H$_2$O (2b). As above for **1a**. Yield: 46 mg (0.04 mmol), 34%. ^{1}H NMR in CD$_3$CN at 298 K, δ/ppm: 10.09 [1H, d, H6(B)], 8.56−8.63 [1H, d, H3(B)], 8.50−8.55 [1H, d, H3'], 8.38−8.44 [1H, d, H3''], 8.27−8.37 [1H, d, H3], 8.15−8.23 [2H, m, H4', H5'], 8.06−8.13 [1H, t, H4(B)], 7.86−7.95 [3H, m, H4'', H6'', H4], 7.78−7.85 [1H, t, H5(B)], 7.60−7.68 [1H, d, H6], 7.47−7.52 [1H, t, H5''], 7.37−7.46 [1H, d, H6(A)], 7.25−7.36 [1H, t, H4(A)], 7.15−7.23 [1H, t, H5], 6.95−7.05 [1H, t, H5(A)], 6.4 [1H, d, H3(A)]. MS. Found 556.2 (M^{2+}); Calcd: 556. Elemental analysis for OsRuC$_{47}$H$_{19}$D$_{16}$N$_{12}$-ClP$_2$F$_{12}$·H$_2$O: Calcd: C 39.8%, H 2.61%, N 11.85%. Found: C 39.7%, H 2.66%, N 11.77%.

Instrumental Methods. ^{1}H NMR spectra were recorded on a Bruker Advance 400 MHz NMR spectrometer. All measurements were carried out in CDCl$_3$ for ligands and in d$_3$-acetonitrile for complexes. Data are relative to residual solvent. UV/vis absorption spectra were recorded on a JASCO 570 UV/vis/NIR or a JASCO 600 UV/vis spectrophotometer using a 1 cm path length quartz cells. Absorption maxima are ± 2 nm: molar absorptivities are ± 10%. Emission spectra were recorded at 298 K in 10 mm path length cells on a JASCO-7200 spectrofluorimeter equipped with a red sensitive Hamamatsu R928 detector. The excitation source is corrected between 200 and 600 nm. Emission spectra are not corrected for detector response. The emission lifetimes were determined by means of a

Time Correlated Single Photon Counter using an Edinburgh Instruments nf900 ns flashlamp and CD900 TAC. Solvent was Uvasol grade acetonitrile. Emission lifetimes (±5%) were calculated using a single exponential fitting function. Mass spectra were recorded on a Bruker-EsquireLC_00050 mass spectrometer using electrospray ionization with positive polarity and a cap-exit voltage of 167 V. Spectra were recorded in the scan range of 50−2200 m/z with an acquisition time of between 300 and 900 μs and a potential of between 30 and 70 V. Each spectrum was recorded by the summation of 20 scans. Electrochemical measurements were carried out with analyte concentrations of typically 0.5−1.0 mM in anhydrous CH$_3$CN with 0.1 M tetrabutylammonium hexafluorophosphate (TBAPF$_6$) using a CH Instruments Version 6.24 software controlled potentiostat (CHI 750C). A glassy carbon electrode, Pt wire and saturated calomel electrode (SCE) were used as working, counter and reference electrodes, respectively. Prior to each experiment the solutions were deoxygenated with argon and a blanket of argon was maintained during analysis. Spectroelectrochemistry was carried out in both UV/vis and NIR regions using a model 760c potentiostat (CH Instruments). Platinum gauze working electrode (Aldrich), Pt wire auxiliary electrode, and an SCE were used as the working, counter and reference electrodes, respectively. A custom-made 2 mm path length 1.2 mL volume quartz cuvette was employed for all spectroelectrochemical measurements. UV/vis/NIR spectra were recorded on a JASCO 570 UV/vis/NIR spectrophotometer.

Raman spectra were obtained with excitation at 400.8 (50 mW at source, PowerTechnology), 449 nm (35 mW at source, PowerTechnology), 473 (100 mW at source, Cobolt Lasers), 532 nm (300 mW at source, Cobolt Lasers), 561 nm (100 mW at source, Cobolt Lasers), and 355 nm (10 Hz 3 mJ per pulse, Spitlight 200, Innolas) to the sample through a 5 cm diameter plano convex lens ($f = 6$ cm) and Raman scattering collected in a 180° backscattering arrangement. The collimated Raman scattering was focused by a second 5 cm diameter plano-convex lens ($f = 6$ cm) through an appropriate long pass edge filter (Semrock) into a Shamrock300 spectrograph (Andor Technology) with a 1200 L/mm grating blazed at 500 nm and collected by a Newton EMCCD (Andor Technology) operating in conventional ccd mode. Data were recorded and processed using Solis (Andor Technology) with spectral calibration performed using the Raman spectrum of acetonitrile/toluene 50:50 (v:v). Samples were held in quartz 10 mm path length cuvettes.

Analytical High Performance Liquid Chromatography (HPLC) experiments were carried out using an analytical HPLC system consisting of a Varian Prostar HPLC pump fitted with a 20 μL injection loop, a Varian Prostar PDA detector connected to a dedicated PC, and a HiChrom Partisil P10SCX-3095 cation exchange column. The mobile phase used was acetonitrile:water 80:20 (v:v) containing 0.01−0.08 M LiClO$_4$; the flow rate was 2.0 cm^3/min. The monitoring wavelength used was 280 nm. Photostability of complexes **1a**/**2a** was monitored by HPLC. Samples were irradiated at 470 nm with a 9 W LED-array.

Results and Discussion

Synthesis. The dinuclear complexes **1a**/**1b** and **2a**/**2b** were prepared by addition of the soluble mononuclear complexes [Ru(bpy)$_2$(bpt)]$^+$/[Ru(d$_8$-bpy)$_2$(bpt)]$^+$ and [Os(bpy)$_2$(bpt)]$^+$/[Os(d$_8$-bpy)$_2$(bpt)]$^+$, respectively, to a solution containing the mononuclear complex Ru-(tpy)Cl$_3$ in EtOH/H$_2$O followed by heating at reflux and isolation by chromatography.

^{1}H NMR Spectroscopy. The ^{1}H NMR spectroscopic and mass spectral data for the mononuclear complexes are in agreement with previous reports.[13] For the dinuclear complexes the availability of **1b** and **2b** allow for analysis of the proton chemical shifts in bpt$^-$ and tpy

Table 1. Spectroscopic and Electrochemical Data for Complexes **1a** and **2a** and Related Analogues[a]

	absorption λ_{max} /nm ($\varepsilon/10^4$ M^{-1} cm^{-1})	emission[a] λ_{max} /nm	τ/ns[a]	V vs SCE [ΔEp /mV]
1a	428 (0.95), 467 (1.55), 520 (sh)	757	58	0.72 [65], 1.19 [60]
2a	488 (0.69), 608 (0.40)	768	13	0.65 [65], 0.86 [60]
[Ru(bpy)$_2$(bpt)]$^+$ [b,c]	475 (1.13)	678	160	0.85
[Os(bpy)$_2$(bpt)]$^+$ [c,d]	486 (1.08), 610 (0.28)	762	55	0.49
[Ru(tpy)(phen)Cl]$^+$ [e]	380, 439(0.60), 502(0.93)	710		0.78
[Ru(bpy)$_2$(bpt)Ru(bpy)$_2$]$^{3+}$ [b,c]	453 (2.26)	648	100	1.04, 1.34
[Os(bpy)$_2$(bpt)Os(bpy)$_2$]$^{3+}$ [d]	460 (1.82), 475 (1.82), 600 (0.44)	756	30	0.64, 0.85
[Os(bpy)$_2$(bpt)Ru(bpy)$_2$]$^{3+}$ [d]	453 (2.37), 580 (sh), 670 (sh)	762	25	0.65, 1.30

[a] Solutions purged with Ar at 298 K. [b] From ref 13. [c] From ref 15. [d] From ref 14. [e] From ref 30.
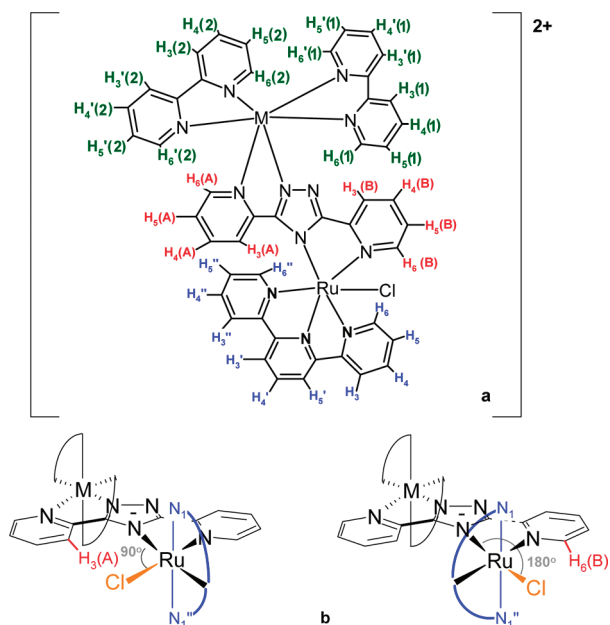
Figure 2. Numbering scheme used for the protons (a) and the structures of the two possible isomers (b) for the dinuclear complexes **1a** and **2a**. The proximity of the chlorido ligand to H3(A) and H6(B), respectively, used to identify the structure of the isolated complexes. Blue lines indicate the tpy ligand.

Figure 3. ^{1}H NMR spectra of (upper) [Ru(d$_8$-bpy)$_2$(bpt)Ru(tpy)Cl]$^{2+}$ **1b** and [Os(d$_8$-bpy)$_2$(bpt)Ru(tpy)Cl]$^{2+}$ **2b**, in CD$_3$CN.

ligands. The coordination mode of the Ru(tpy)Cl- unit in **1** and **2** can, potentially, be such that the chlorido ligand is trans to either the triazolato or the pyridyl ring of the bpt$^-$ bridging ligand (Figure 2b).

The ^{1}H NMR spectra of **1b** and **2b** are shown in Figure 3. Further ^{1}NMR and COSY spectra are shown in Supporting Information, Figures S1−S3. ^{1}H COSY NMR spectroscopy together with comparison of the chemical shifts with those of related complexes allows for assignment of the absorptions of the bpt and tpy ligands.

From the analysis of the ^{1}H NMR spectra of the isotopologues **1b** and **2b** (Figure 3) it is apparent that only one geometric isomer, where the chlorido ligand is trans to the triazolato ring of the bpt$^-$ ligand, is isolated. This assignment is based on the downfield shifted doublet at about 10.1 ppm with a coupling constant J of 5.6 Hz for both **1b** and **2b** (Figure 3). The chemical shift and the corresponding coupling constant indicate through-space interaction between an H6 type proton of a pyridine ring of the bpt$^-$ and the chlorido ligand. In the case of the chlorido ligand being cis to the triazolato ligand then the H3(A) ligand would be influenced by the chlorido ligand with a chemical shift similar to that observed but with a larger coupling constant (7−9 Hz). Further support for
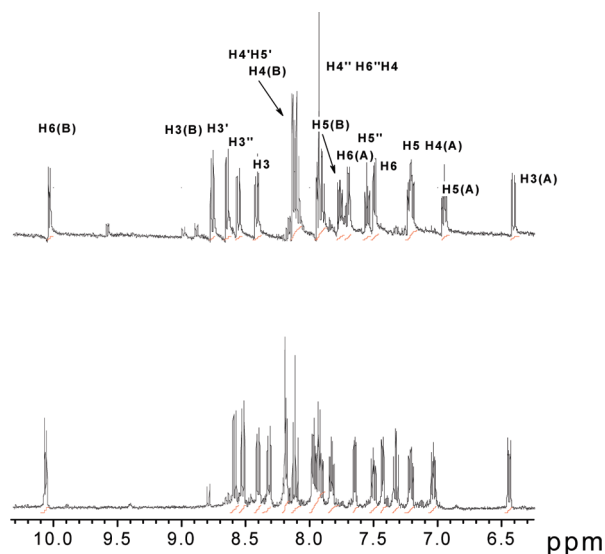
this assignment is the upfield shift of the H3(A) resonance at about 6.40 ppm (J = 8.0 Hz) because of shielding by the ring current of the tpy ligand.

Examination of the resonances of the tpy ligand in complexes **1** and **2** gives additional support for this structural assignment. The protons Hn and Hn$''$ on the py rings of the tpy ligand are not chemically equivalent in complexes **1** and **2**. This is shown by the fact that the chemical shifts of H3 and H3$''$, H5 and H5$''$, and H6 and H6$''$, are different. This asymmetry indicates that the chlorido ligand is not equidistant to the two pyridyl rings of the tpy ligand, that is, it does not lie in the plane formed from the Ru−N bonds with the pyridyl and triazolato rings of the bpt$^-$ ligand and hence the Ru(tpy)Cl center is in a distorted octahedral geometry.

UV/vis Absorption and Emission Spectroscopy. Electronic absorption and emission data for the mononuclear and dinuclear complexes are listed in Table 1. All complexes exhibit absorption and emission properties that are characteristic of ruthenium(II) and osmium(II) based polypyridyl complexes with triazolato containing bridging ligands.

The absorption spectra for **1a** and **2a** are shown in Figure 4. In the UV region (< 350 nm) the absorptions are assigned to $\pi-\pi*$ intraligand electronic transitions associated with the bpy, tpy, and bridging triazolato ligands,[1,13] whereas those in the visible region (400−570 nm) are assigned to ^{1}MLCT (metal ligand charge transfer) transitions.[1] The shoulder at about 525 nm is typical for
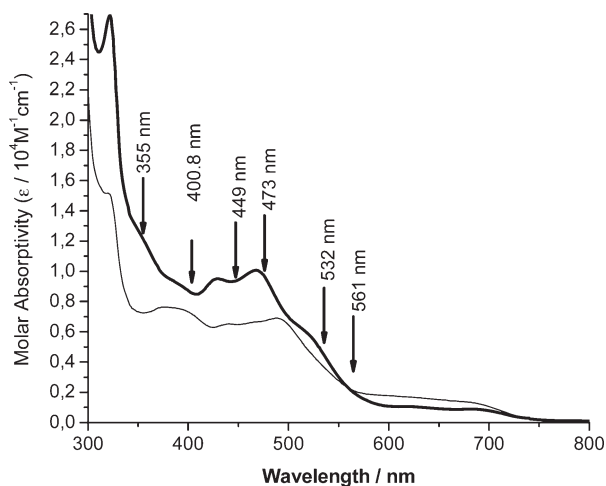
Figure 4. Absorption spectra of **1a** [Ru(bpy)$_2$(bpt)Ru(tpy)Cl]$^{2+}$ (thin line) and [Os(bpy)$_2$(bpt)Ru(tpy)Cl]$^{2+}$ **2a** (black line) in CH$_3$CN. Laser excitation lines used for acquiring Raman spectra are indicated with arrows.
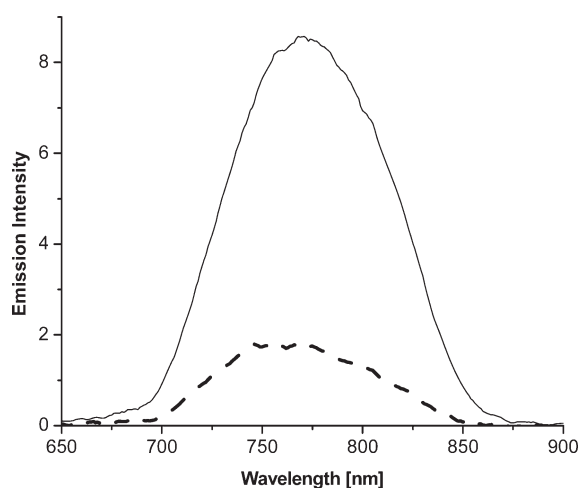

Figure 5. Emission spectra of **1a**[Ru(bpy)$_2$(bpt)Ru(tpy)Cl]$^{2+}$ (dashed line, λ_{exc} 482 nm) and [Os(bpy)$_2$(bpt)Ru(tpy)Cl]$^{2+}$ **2a** (solid line λ_{exc} 468 nm) in CH$_3$CN. The absorbance of the two solutions at the excitation wavelengths were the same. The concentrations were approximately $1-2 \times 10^{-5}$ M.

ruthenium(II)(N5)chlorido complexes.[28] The absorptions > 570 nm are assigned to ^{3}MLCT transitions in the case of **2a**; however, for **1a** a significant absorption is observed in this region also, which are reminiscent of the absorption spectrum of [Ru(tpy)$_2$]$^{2+}$.[29] These assignments are supported by resonance Raman spectroscopy (vide infra).

The emission spectra of both **1a** and **2a** show maxima at 757 and 768 nm, respectively (Figure 5). In both cases the emission energy and lifetime (Table 1) is typical of emission from a ^{3}MLCT excited state, localized either on a bpy or on a tpy ligand. The near coincidence in energy of the emission of the two complexes could suggest that the

emission is localized at the same metal center for both complexes, that is, the [Ru(tpy)Cl]$^+$ center. However, the differences in emission lifetimes and intensities indicate otherwise. For **1a**, the emissive ^{3}MLCT state is assigned to be localized on the [Ru(tpy)Cl]$^+$ moiety on the basis that the related complex[13,15] [Ru(bpy)$_2$(bpt)Ru(bpy)$_2$]$^{3+}$ has an emission maximum at 648 nm (Table 1). The lifetime of the emission of **1a** is considerably longer (58 ns) than that expected for compounds such as [Ru(tpy)(phen)Cl]$^+$ for which the lifetimes are < 1 ns[30] and is closer to that of [Ru(bpy)$_2$(bpt)Ru(bpy)$_2$]$^{3+}$ (100 ns);[15] however, the substitution of the bpy ligand of [Ru(tpy)(bpy)Cl]$^+$ with the strongly σ-donating triazolato ligand will raise the energy of the ^{3}MC excited state which is typically the major excited state deactivation channel for ruthenium(II) polypyridyl complexes.[1] In the case of **2a** the shorter lifetime of the emission (13 ns) and the similarity in emission energy to the related complexes[15] [Os(bpy)$_2$(bpt)Os(bpy)$_2$]$^{3+}$ and [Os(bpy)$_2$(bpt)Ru(bpy)$_2$]$^{3+}$ suggests that the emissive excited state is localized on the Os(bpy)$_2$ moiety. Furthermore, the relatively higher intensity of emission for **2a** over **1a** despite the shorter excited state lifetime (Figure 5) indicates that **2a** has a shorter radiative lifetime in accordance with a switch from a ruthenium(tpy) to an osmium(bpy) centered emission between **1a** and **2a**.

Photostability. Previously it was shown for complexes of the type [Ru(bpy)$_2$(L)Cl]$^+$ where L = pyridine,[31] 4-vinyl-imidazole[32] and poly-4-vinyl-pyridine,[33] that rapid loss of a chlorido ligand can be observed by photochemical or thermal activation and photoinduced ligand loss has been observed for [Ru(tpy)(bpy)Cl]$^+$ also.[28a] The photostability under visible excitation of **1a** and **2a** in acetonitrile was determined by HPLC. Formation of a main photolysis product is detected only on extended photolysis after 48 and 72 h irradiation for **1a** and **2a**, respectively. This product manifests itself in the appearance of a peak in the HPLC chromatogram at a retention time longer than observed for **1a** and **2a** (see Figures S4 and S5 in Supporting Information), which indicates that the photoproduct is more positively charged. Comparison of the absorption spectra of **1a** and **2a** and the primary photolysis product indicates the loss of the chlorido ligand (see Supporting Information, Figure S6). This indicates that cleavage of the Ru−Cl bond is unlikely to be significant on the time scale of the absorption and Raman spectroscopic studies (vide infra).

Resonance Raman Spectroscopy. Resonance Raman spectra for compounds **1a/1b** and **2a/2b** were recorded in acetonitrile solution at room temperature upon excitation at 355, 400.8, 449, 473, 532, and 561 nm (see Figure 4 for absorption spectra). Isotopic labeling indicates that between 400 and 473 nm the Raman spectra are dominated by resonance enhanced bands from vibrational modes of the bpy (Figure 6). At 532 nm, the Raman spectrum shows contributions from vibrational modes

(28) (a) Suen, H. F.; Wilson, S. W.; Poimerantz, M.; Walsh, J. L. *Inorg. Chem.* **1989**, *28*, 786–791. (b) Patra, S.; Sarkar, B.; Ghumaan, S.; Patil, M. P.; Mobin, S. M.; Sunoj, R. B.; Kaim, W.; Lahiri, G. K. *Dalton Trans.* **2005**, 1188–1194.
(29) Coe, B. J.; Thompson, D. W.; Culbertson, C. T.; Schoonover, J. R.; Meyer, T. J. *Inorg. Chem.* **1995**, *34*, 3385–3395.

(30) Bonnet, S.; Collin, J.-P.; Gruber, N.; Sauvage, J.-P.; Schofield., E. R. *Dalton Trans.* **2003**, 4654–4662.
(31) Clear, J. M.; Kelly, J. M.; Pepper, D. C.; Vos, J. G. *Inorg. Chim. Acta* **1979**, *33*, L139–L140.
(32) Geraty, S.; Vos, J. G. *J. Electroanal. Chem.* **1984**, *176*, 389–393.
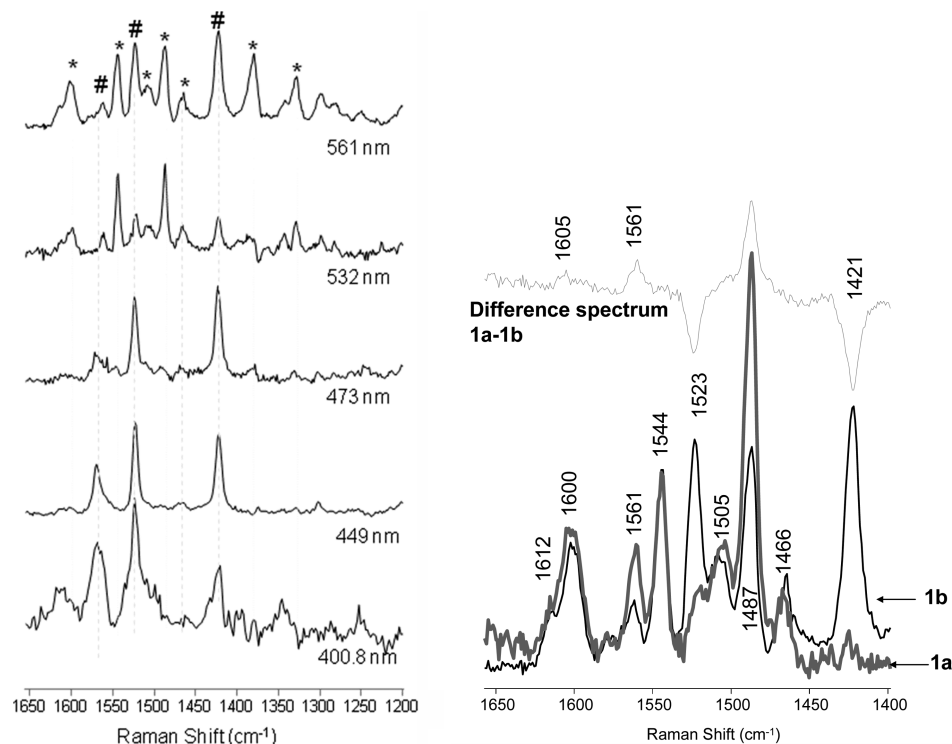(33) Haas, O.; Kriens, M.; Vos, J. G. *J. Am. Chem. Soc.* **1981**, *103*, 1318–1319.

Figure 6. (Left) Resonance Raman spectra in CH_3CN of $[Ru(d_8\text{-}bpy)_2(bpt)Ru(tpy)Cl]^{2+}$ **1b** at selected excitation wavelengths. (Right) Resonance Raman spectra in CH_3CN of $[Ru(bpy)_2(bpt)Ru(tpy)Cl]^{2+}$ **1a** and $[Ru(d_8\text{-}bpy)_2(bpt)Ru(tpy)Cl]^{2+}$ **1b** at 561 nm. The difference spectrum (**1a-1b**) shows the characteristic Raman bands of h_8- and d_8-bpy. Solvent signals were subtracted. The * indicates tpy bands, and the # indicates d_8-bpy bands.

assignable to the other ligands, for example, tpy,[34] (1612, 1600, 1561, 1544, 1505, 1487, 1466 cm^{-1}) in addition to the characteristic bpy bands. Notably the relative contribution of bpy features[35] in the spectrum recorded at 561 nm is much greater than at 532 nm, indicating that bpy based MLCT states contribute to the red part of the absorption spectrum significantly. This suggests that the absorptions at the red edge of the visible absorption spectrum are dominated by ^{1}MLCT $-(M^{II}\text{-}tpy)$ with the more intense ^{1}MLCT $-(M^{II}\text{-}bpy)$ transitions dominating the spectrum between 400 and 500 nm (where M^{II} = Ru^{II} or Os^{II}).

The surface enhanced Raman spectra of **2a/2b** on gold colloid at 785 nm are shown in Figure S7 in the Supporting Information. Bands assignable to bpy ligands are readily identified on the basis of the effect of isotopic substitution and are in agreement with expected values.[35] Resonance Raman spectra obtained under ns-pulsed excitation at 355 nm show a distinct difference between the homo- (**1a/1b**) and hetero-(**2a/2b**) dinuclear complexes (Figure 7). In all cases bands at 1603 and 1558 cm^{-1} are observed; however, a band at 1518 cm^{-1} is observed only in the case of the d_8-bpy labeled complexes. For **2a** and **2b** bands assignable to the h_8-bpy and d_8-bpy anion radical of a bpy based ^{3}MLCT state are observed, respectively. For **1a** and **1b** similar excited state features are not
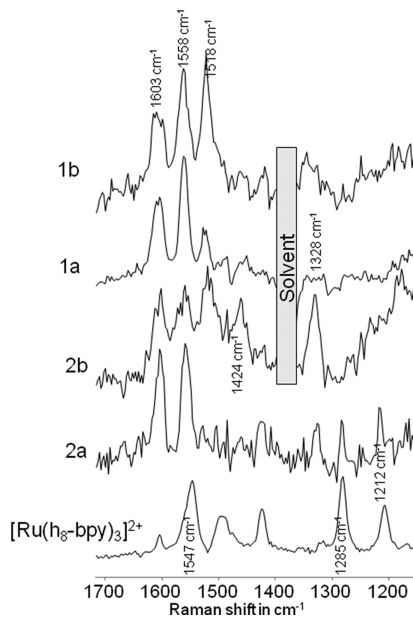

Figure 7. Transient resonance Raman spectra in CH_3CN of $[Ru(bpy)_3]^{2+}$, $[Ru(bpy)_2(bpt)Ru(tpy)Cl]^{2+}$ **1a**, $[Ru(d_8\text{-}bpy)_2(bpt)Ru(tpy)Cl]^{2+}$ **1b**, $[Os(bpy)_2(bpt)Ru(tpy)Cl]^{2+}$ **2a**, and $[Os(bpy)_2(bpt)Ru(tpy)Cl]^{2+}$ **2b** at 355 nm (7 ns pulse width, 10−15 mJ per pulse). Solvent signals are subtracted.

observed. It should be noted that the $\pi-\pi^*$ transition of tpy is red-shifted with respect to that of bpy, and hence the tpy anion radical absorption will be expected to undergo a similar red-shift and will be out of resonance with the 355 nm excitation line. The data support the assignment of excited state localization made on the basis of emission spectroscopy (*vide supra*).

(34) Bhuiyan, A. A.; Kincaid, J. R. *Inorg. Chem.* **1998**, *37*, 2525–2530.

(35) (a) Mallick, P. K.; Danzer, G. D.; Strommen, D. P.; Kincaid, J. R. *J. Phys. Chem.* **1988**, *92*, 5628–5634. (b) Strommen, D. P.; Mallick, P. K.; Danzer, G. D.; Lumpkin, R. S.; Kincaid, J. R. *J. Phys. Chem.* **1990**, *94*, 1357–66. (c) Mallick, P. K.; Strommen, D. P.; Kincaid, J. R. *J. Am. Chem. Soc.* **1990**, *112*, 1686–1690. (d) Manuel, D. J.; Strommen, D. P.; Bhuiyan, A.; Sykora, M.; Kincaid, J. R. *J. Raman Spectrosc.* **1997**, *28*, 933–938.
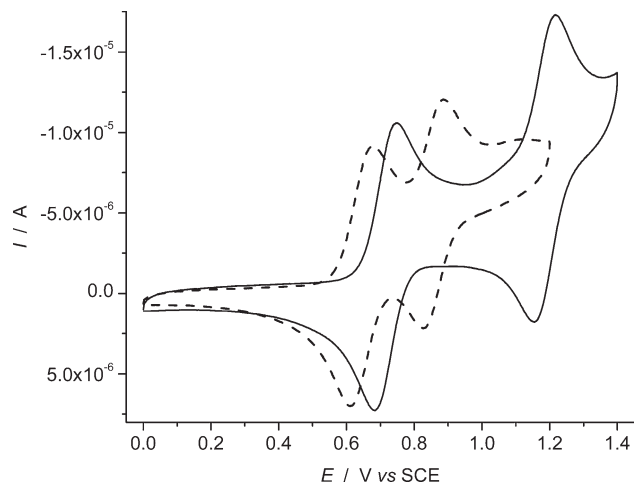
Figure 8. Cyclic voltammograms of $[Ru(bpy)_2(bpt)Ru(tpy)Cl]^{2+}$ **1a** (solid line) and $[Os(bpy)_2(bpt)Ru(tpy)Cl]^{2+}$ **2a** (dashed line) in 0.1 $TBAPF_6/CH_3CN$.

Electrochemical Properties. The redox properties of dinuclear complexes **1a** and **2a** are detailed in Table 1. Two reversible oxidative processes are observed for each complex, both of which are assigned to one-electron metal-centered oxidations (Figure 8).

The potential of the first oxidation step of the dinuclear complex **1a** is different than the value obtained for the related dinuclear compounds[13] $[Ru(bpy)_2(bpt)Ru(bpy)_2]^{3+}$ (Table 1). For **1a** (0.72 V vs SCE) the first oxidation is significantly less positive than for the related complex[13] $[Ru(bpy)_2(bpt)Ru(bpy)_2]^{3+}$ (1.04 V). The first oxidation of **1a** can be assigned to the $[Ru(tpy)Cl]^+$ moiety by comparison with the mononuclear complex $[Ru(tpy)(phen)-Cl]^+$ (0.78 V vs SCE).[30] The less positive potential of the second oxidation of **1a** compared with[13] $[Ru(bpy)_2(bpt)-Ru(bpy)_2]^{3+}$ reflects the increased electron density on the $Ru^{III}(tpy)Cl$ moiety compared with a $Ru^{III}(bpy)_2$ moiety (i.e., lower redox potential in the case of the former). The reductive electrochemistry of **1b** is shown in Figure S8 (see Supporting Information). Several reduction processes are observed at potentials typical of those of polypyridyl complexes; however, an irreversible reductive process at about −1.2 V versus SCE serves to distort the remaining reduction processes precluding a detailed analysis; similar reductive electrochemistry is observed for all complexes.

For complex **2a** the first oxidation is at the same potential (Figure 8) as the first oxidation of dinuclear complex[14] $[Os(bpy)_2(bpt)Ru(bpy)_2]^{3+}$ (Table 1) and is assigned (*vide infra*) to the $Os(bpy)_2$- moiety. The second oxidation of **2a** (0.86 V) is higher than the first oxidation of **1a** (0.72 V) indicating that the $Os^{III}(bpy)_2$ center reduces the σ-donor properties of the triazolato ligand compared with the $Ru^{II}(bpy)_2$ moiety in **1a**. The oxidation potential of Ru^{II} center of **2a** is comparable with that of the mononuclear complex[30] $[Ru(bpy)(tpy)Cl]^+$ (Table 1) as expected on the basis of the reduced σ-donor ability of the triazolato unit in **2a**$^+$ than in **1a**.

Spectroelectrochemistry. Bulk electrolysis at 0.80 and 0.70 V for **1a** and **2a**, respectively, generates the mixed valence state. The fully oxidized state is obtained by electrolysis 1.35 V for **1a** and 0.95 V for **2a** (Figure 9). For complex **1a** the formation of a mixed valence state is

manifested in the decrease in the intensity of the ^{1}MLCT absorption bands at 21000 cm^{-1} (475 nm) and the appearance of a broad absorption band centered at 11000−17000 cm^{-1} and at 7100 cm^{-1}. Notably for **1a** the first oxidation leads to a loss in intensity of the ^{1}MLCT absorption above 500 nm with minimal effect on the intensity at about 450 nm. This indicates that Ru-tpy ^{1}MLCT absorptions are absent in the mixed valence complex and hence that the first oxidation is localized predominantly on the Ru(tpy) moiety. Oxidation of the complex to the $Ru^{III}Ru^{III}$ state results in a disappearance of the absorption at 7100 cm^{-1} and a further decrease in the ^{1}MLCT bands at 21000 cm^{-1}. The disappearance of the 7100 cm^{-1} band upon full oxidation supports the assignment of the band as an metal to metal charge transfer (MMCT) transition.

Oxidation of **2a** at 0.70 V to form the $Os^{III}Ru^{II}$ redox state results in a decrease in intensity of the ^{1}MLCT absorptions at 20000 and 22500 cm^{-1}, and the ^{3}MLCT absorption (13000−17000 cm^{-1}). These changes are accompanied by the appearance of an absorption band at 6000 cm^{-1}. The latter feature is assigned to an MMCT transition on the basis of its subsequent disappearance upon oxidation of the second metal center at 0.95 V. In addition to a decrease in the MMCT band, the MLCT bands decrease further in the fully oxidized state (Figure 9).

Charge Transfer Band Analysis. The delocalization parameter (α^2) and the electronic coupling constant (H_{ab}) were calculated for **1a** and **2a** with eqs 1 and 2 from the spectroelectrochemical data (Table 2).[36]

$$\alpha^2 = \frac{(4.2 \times 10^{-4})\varepsilon_{max}\Delta\nu_{1/2}}{d^2 E_{op}} \qquad (1)$$

$$H_{ab} = [\alpha^2 E_{op}^2]^{1/2} \qquad (2)$$

where ε_{max} is the molar absorptivity of the MMCT band ($M^{-1} cm^{-1}$), $\Delta\nu_{1/2}$ is the peak width at half height of the MMCT band (in cm^{-1}), d is the nominal electron transfer distance between the metal centers (6.2 Å for bpt-bridged complexes **1a** and **2a**),[37] and E_{op} is the energy of the MMCT band in cm^{-1}.

Comparison of the delocalization parameters (α^2) (Table 2) shows that **1a** and $[(Ru(bpy)_2)_2bpt]^{3+}$ have the highest values of electronic delocalization among the bpt−bridged complexes in the mixed valence state. This is ascribed to the more effective overlap between the dπ orbitals of the Ru(III) center and a σ-orbital of the triazolato with respect to that of the dπ orbitals of the Os(III). Moreover, the larger electronic coupling in the mixed valence states of homobinuclear ruthenium

(36) Hush, N. S. *Electrochim. Acta* **1968**, *13*, 1005–1023.

(37) The use of the value 0.62 nm for the electron transfer distance is made on the basis of consistency with previous studies on related systems. Given the similarity in terms of the coordination environment and solvent condition employed in obtaining the absorption spectra of the mixed valence species, the inherent error in the value of *d* will be constant for all complexes considered in the present study. It should be noted that the electron transfer distance has been subject to extensive discussion in the literature in particular with respect to delocalization of the donor and acceptor orbitals. See for example: (a) Bublitz, G. U.; Laidlaw, W. M.; Denning, R. G.; Boxer, S. G. *J. Am. Chem. Soc.* **1998**, *120*, 6068–6075. (b) Browne, W. R.; Hage, R.; Vos, J. G. *Coord. Chem. Rev.* **2006**, *250*, 1653–1668 and references therein.
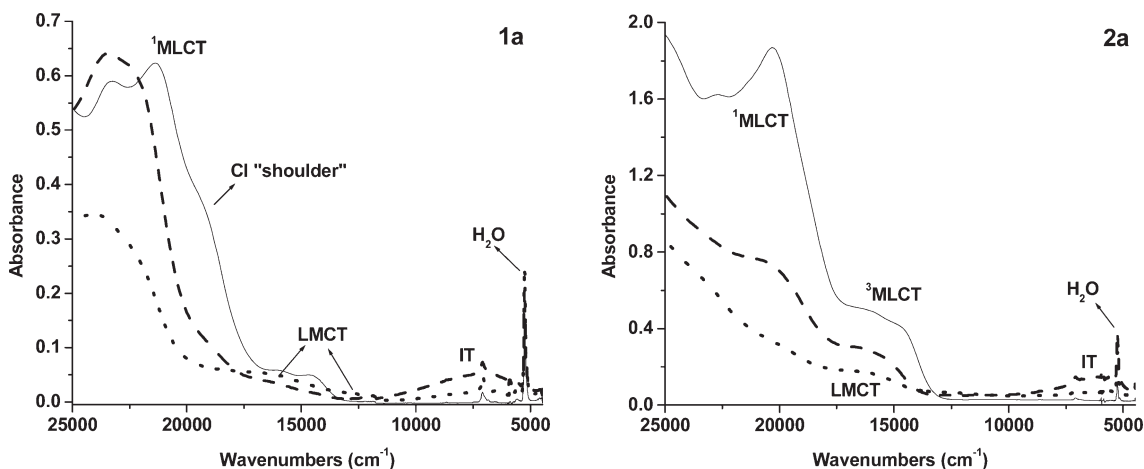
Figure 9. UV/vis/NIR absorption spectra of the dinuclear complexes **1a**[Ru(bpy)$_2$(bpt)Ru(tpy)Cl]$^{2+}$ (left) and [Os(bpy)$_2$(bpt)Ru(tpy)Cl]$^{2+}$ **2a** (right) in the M$_2^{II,II}$ (solid lines), M$_2^{II,III}$ (dashed lines), and M$_2^{III,III}$ (dotted lines) redox states.

Table 2. Spectroelectrochemical Data for **1a** and **2a** and Related Complexes[a]

	E_{op}[b]/cm^{-1}	ε_{max}/M^{-1} cm^{-1}	α^2	H_{ab}	ΔE[c]/mV	$\Delta\nu_{1/2calc}$/cm^{-1}	$\Delta\nu_{1/2}$/cm^{-1}	ref
1a	7100	1266	0.0102	716	470	3910	5200	
2a	6000	538	0.0046	406	210	3650	4660	
[(Ru(bpy)$_2$)$_2$bpt]$^{3+}$	5556	2452	0.0160	702	300	3341	3300	14
[(bpy)$_2$Ru(bpt)Os(bpy)$_2$]$^{3+}$	7143	1198	0.0070	598	470	3650	3800	14
[(bpy)$_2$Os(bpt)Ru(bpy)$_2$]$^{3+}$	8772	1133	0.0061	685	650	3700	4300	14
[(Os(bpy)$_2$)$_2$bpt]$^{3+}$	8333	455	0.0027	433	210	4170	4500	14

[a] In CH$_3$CN. [b] E_{op} and $\Delta\nu_{1/2}$ are ± 100 cm^{-1}. [c] ΔE = ±20 mV.

complexes **1a** and [(Ru(bpy)$_2$)$_2$bpt]$^{3+}$ than either of the heteronuclear complexes **2a**, [(bpy)$_2$Ru(bpt)Os(bpy)$_2$]$^{3+}$ and [(bpy)$_2$Os(bpt)Ru(bpy)$_2$]$^{3+}$, indicates that such a larger intermetallic delocalization takes place through a dπ(Ru^{III})-π(L) orbital mixing (highest occupied molecular orbital (HOMO) mediated superexchange) rather than dπ(Ru^{II})- π*(L) mixing (lowest unoccupied molecular orbital (LUMO) mediated superexchange). Analogously, the electronic coupling constants H_{ab} follow the same trend with the strongest coupling seen for the homobinuclear Ru complexes (Table 2). The determination of the type of metal-to-metal interaction in binuclear complexes is obtained from the comparison between the $\Delta\nu_{1/2}$ obtained from spectroelectrochemical data and the value $\Delta\nu_{1/2calc}$ determined from correlation of spectroelectrochemical and electrochemical data (eq 3).

$$\Delta\nu_{1/2calc} = [2310(E_{op} - \Delta E)]^{1/2} \qquad (3)$$

where ΔE is the difference between the oxidation potentials of the metal centers in the binuclear complex (redox asymmetry[38]). In case of complexes **1a** and **2a** the value of $\Delta\nu_{1/2}$ determined directly from spectroelectrochemical data is larger than that calculated $\Delta\nu_{1/2calc}$ (Table 2), indicating that the system is best described as Type II (valence localized, M^{II}M^{III}) in the classification proposed

by Robin and Day.[39] However, it should be noted that the use of ΔE, the difference in redox potentials, must take into account the electrostatic interaction between the metal centers, which can be approximated by the shift in the redox potential of the Ru(tpy) unit between complexes **1** and **2**, if other factors such as changes in backbonding and so on are ignored. From Table 1 this is calculated to be 140 mV, and hence the contributions from inherent difference in redox potentials between the metal centers are 330 mV and 70 mV and $\Delta\nu_{1/2calc}$ 3955 and 3700 cm^{-1} for **1** and **2**, respectively. Hence, even though these values are greater than in Table 2 with this correction the complex is still best described as valence localized.

Conclusions

Here, the synthesis, ^{1}H NMR, absorption, emission, and Raman spectral, spectroelectrochemical, and electrochemical characterization of the dinuclear complexes [(bpy)$_2$Ru(bpt)-Ru(tpy)Cl]$^{2+}$ (**1a**) and [(bpy)$_2$Os(bpt)Ru(tpy)Cl]$^{2+}$ (**2a**) have been described together with their deuterated isotopologues **1b/2b**. ^{1}H NMR spectroscopy indicates that only one isomer is isolated for both **1b** and **2b** in which the chlorido ligand is trans to the triazolato ligand. Both complexes **1a** and **2a** are relatively photostable in contrast to related mononuclear chlorido containing systems. Emission and resonance Raman spectroscopy indicate that for compounds **1a/1b** the emissive excited state is localized on the [Ru(tpy)Cl] center, whereas for **2a/2b** the emissive state is localized on the Os(bpy)$_2$ unit. Electrochemistry and UV/vis/NIR spectroelectrochemistry

(38) It should be noted that the use of redox asymmetry, i.e., the difference in redox potential, to assess the degree of internuclear interaction in terms of delocalization is not advisable even in the case of fully symmetric systems, as the electrostatic contribution to asymmetry can be significant. In the present study the inherent asymmetry due to differences in the coordination environment of the metal centers contributes the most to redox asymmetry with delocalization and internuclear interaction making a second order contribution.

(39) (a) Robin, M. B.; Day, P. *Adv. Inorg. Chem. Radiochem.* **1967**, *10*, 247–422. (b) Demadis, K. D.; Hartshorn, C. M.; Meyer, T. J. *Chem. Rev.* **2001**, *101*, 2655–2685.

of **1a** and **2a** show that internuclear interaction in the mixed valence states is via bridging ligand HOMO mediated superexchange and that the site of the first oxidation switches from the M(tpy)Cl- unit to the M(bpy)$_2$- unit on going from **1a** to **2a**.

These systems show that the "direction" of energy and electron transfer in a multinuclear complex can be controlled by the switching of the metal center from Ru to Os and opens up considerable opportunities in application of these systems to molecular based electronic and photonic devices.

Supporting Information Available: ^{1}H NMR spectra of [Ru(bpy)$_2$(bpt)]$^+$, [Ru(d$_8$-bpy)$_2$(bpt)]$^+$, [Ru(bpy)$_2$(bpt)Ru(tpy)Cl]$^{2+}$, and [Os(bpy)$_2$(bpt)Ru(tpy)Cl]$^{2+}$, COSY Spectrum for [Os(d$_8$-bpy)$_2$(bpt)Ru(tpy)Cl]$^{2+}$. HPLC chromatograms of [Ru(bpy)$_2$(bpt)Ru(tpy)Cl]$^{2+}$ and [Os(bpy)$_2$(bpt)Ru(tpy)Cl]$^{2+}$ before and after irradiation; normalized absorption spectra of **1a** and **2a** before and after irradiation; surface enhanced Raman spectra (Au colloid in water) of **2a**/**2b**. This material is available free of charge via the Internet at http://pubs.acs.org.